IEEE Open Journal of Vehicular Technology

Received 23 August 2023; accepted 2 October 2023. Date of publication 13 October 2023;
date of current version 23 October 2023. The review of this article was coordinated by Editor Haiping Du.

Digital Object Identifier 10.1109/OJVT.2023.3323626

Probabilistic Assessment of Community-Scale Vehicle Electrification Using GPS-Based Vehicle Mobility Data: A Case Study in Qatar

FULIN FAN [1,2], I. SAFAK BAYRAM [2] (Senior Member, IEEE), USMAN ZAFAR [3] (Member, IEEE), SERTAC BAYHAN [3] (Senior Member, IEEE), BRUCE STEPHEN [2] (Senior Member, IEEE), AND STUART GALLOWAY [2] (Member, IEEE)

[1]School of Electrical Engineering and Automation, Harbin Institute of Technology, Harbin 150001, China
[2]Department of Electronic and Electrical Engineering, University of Strathclyde, G1 1XW Glasgow, U.K.
[3]Qatar Environment and Energy Research Institute, Hamad Bin Khalifa University, Doha 5825, Qatar

CORRESPONDING AUTHOR: SERTAC BAYHAN (e-mail: sbayhan@hbku.edu.qa).

This work was supported in part by Qatar National Research Fund through the National Priorities Research Program under Grant NPRP12S-0214-190083 and in part by Open Access funding provided by the Qatar National Library. The work of I. Safak Bayram was supported by the Royal Society of Edinburgh's Personal Research Fellowship Program.

ABSTRACT To avoid the operational consequence of thermal rating exceedance and the financial consequence of excessive reinforcement, the impact of domestic charging of electric vehicles (EVs) on power distribution networks must be accurately assessed prior to accepting vehicle electrification at the community-scale. Although driven by routine, charging behaviour patterns are also influenced by geography, meteorological conditions and season, hence will have a localised element to them that could reduce the diversity of charging load profiles. To model this uncertainty, this article develops a probabilistic methodology to quantify EV home charging demands based on vehicle mobility data and underlying trip characteristics. Models articulate the departure time distribution using a mixture of von Mises distributions, and incorporate non-negative conditional distributions of trip durations, distances and parking durations, which in turn generalise localised charging behaviours. The resulting load profiles are used to drive a community electric network model based on a distribution feeder in Qatar, a country with high per km energy consumption, to quantify impact scenarios of high temperature and driving habit in terms of voltage and thermal stability. Results indicate that overnight domestic charging is sufficient to support daily trips and local networks are capable of hosting high EV penetration despite peaks.

INDEX TERMS Electric network stability, electric vehicle demand synthesis, probabilistic assessment, vehicle mobility data.

NOMENCLATURE

Abbreviations

BIC	Bayesian inference criterion.
CC-CV	Constant current-constant voltage.
CDF	Cumulative distribution function.
EV	Electric vehicle.
GPS	Global positioning system.
MCMC	Markov chain Monte Carlo.
MLE	Maximum likelihood estimation.
OBD	On-board diagnostic.
PDF	Probability density function.
PV	Photovoltaic.
SoC	State of charge.
SUV	Sport utility vehicle.
TCP	Transmission control protocol.
TPN	Truncated positive normal.
VM	Von Mises.

Symbols

d, d_h	Index of day or hourly segment in a day.
t^{Dep}, t^{Arr}	Time departing from or arriving at home.
T^{D2A}	Duration from t^{Dep} to subsequent t^{Arr}.
T^{A2D}	Duration from t^{Arr} to subsequent t^{Dep}.

D^{Dis}	Travel distance.
f_{vm}	PDF of mixed VM distributions.
N_{vm}	Number of VM components.
p, μ, k	Parameters of mixed VM distributions.
I_0	Modified Bessel function of the first kind of order zero.
f_{tpn}, F_{tpn}	PDF or CDF of mixed TPN distributions.
N_{tpn}	Number of TPN components.
q, λ, σ	Parameters of mixed TPN distributions.
M_{wd}	Number of weekday trip observations.
M_{d_h}	Number of trips departing within d_h.
$\hat{L}$	Maximised Log-likelihood.
C	Clayton copula.
α	Clayton copula parameter.
f_C	Copula-based PDF.

I. INTRODUCTION

There has been an intensified interest in electric vehicles (EVs) to decarbonise the road transport sector, which generates nearly one fourth of the global greenhouse gas emission [1]. In parallel, national EV markets are growing at a faster pace driven by government subsidies and policies aiming to ban the sale of new petrol and diesel cars within a decade (e.g., U.K., France, and Germany [2]). Achieving net-zero in road transport requires sustained effort to expand charging networks and ease the access to charging stations to increase the pace of decarbonisation. This requires vehicle mobility analysis to quantify energy requirements for driving needs and examine daily trips and activities to assess the appropriate locations and types (slow or fast) for EV charging. Electrification of transportation is a global transformational change, as even carbon-rich developing Gulf countries such as Saudi Arabia and Qatar have pledged to introduce EVs and cut road transport emissions [3]. Quantifying the impacts of EV charging on electric networks (e.g., power quality and stability) and planning for the charging infrastructure needs in such countries is a key challenge due to the lack of publicly available datasets (e.g., travel surveys, etc.). To that end, this article presents vehicle mobility analysis using high resolution GPS-traces collected from actual vehicles in Qatar as a case study, develops probabilistic methods to generalise the vehicle mobility data for community-scale EV demand synthesis and evaluates the stability of a typical Qatar distribution network in the context of community-scale vehicle electrification.

The critical input to EV charging planning and impact assessment studies is vehicle mobility data, which is used to analyse spatio-temporal EV demands and charging needs. For instance, drivers who have access to a home charger would not require public fast chargers or workplace charging if the domestic charging is sufficient. On the other hand, for high mileage vehicles or EVs located in densely populated areas, public charging could be the only option. Energy and petrol prices are highly subsidised by the governments in the Gulf region, where residents typically prefer large-engine vehicles and have a higher energy consumption per km than most developed countries [4]. Therefore, electric sport utility vehicle (SUV) models are expected to become popular in transition towards electrified transport.

Most research performs EV mobility analysis either based on national travel surveys that are created with low resolution survey inputs [5], [6], [7] or using high resolution GPS-traces that are collected through cell phone traces or actual on-board recording devices. The advantage of the latter approach is the high resolution and precision of datasets, though the dataset is usually constructed from a limited number of participants [8], [9]. These datasets are then generalised to model the behaviour of larger populations using probabilistic simulation methods (e.g., Markov chain Monte Carlo (MCMC)) and then assess the resulting impacts on electric networks. In [6], U.K. travel surveys are employed as an input to the MCMC method to model the locations and energy demands of EVs, based on which their charging impacts (voltage drops) are quantified at workplaces and rural distribution networks. A similar methodology is followed in [10] which quantifies the peak EV charging load for selected regions based on the National US travel surveys. In [7], vehicle mobility traces are collected from phone traces and a probabilistic location model is developed to estimate the charging needs and locations of vehicles in Bay Area, California, showing that the peak EV charging demands in certain postcodes could be significantly reduced by shifting the location and time of EV charging. In [8], mobility traces of 40 different EVs are collected and analysed with a primary focus to understand their spatio-temporal recharging habits, presenting that most EV drivers use their cars in a very risk-averse way due to range anxiety. In addition, the mobility pattern analysis of petrol vehicles can provide useful insights into how EVs would be used. In [11], mobility analysis is carried out for a single petrol-powered taxi and results are then generalised for the entire fleet, followed by a feasibility analysis which assesses the electrificability rate of the fleet and concludes that more than 75% of the trips can be made with EVs even using small batteries (e.g., 30 kWh). In [12], a similar analysis with a smaller dataset is performed to show how corresponding EVs can be used for daily activities and conclude that EVs with 50 kWh batteries can complete all trips in winter while the minimum battery size should be 64 kWh to complete the same trips in summer due to the effects of hot weather.

Switch to EVs in regions with harsh desert climates is further challenging since the performance of the underlying Lithium-ion battery technology further degrades with high ambient temperature ($> 30\ ^{o}$C). This is mainly because part of the stored energy is used for battery cooling and an increasing energy consumption per km significantly reduces electric driving ranges of EVs, e.g., mostly by $\sim$20% at an ambient temperature of 40 ^{o}C with respect to ideal conditions of 21 ^{o}C [13]. In addition, the fast charge rates (> 50 kW) are limited by the EV's battery management system to maintain battery health and avoid overheating. To that end, EV users may need to stay plugged in for additional hours compared with the EVs located in regions with mild weather.

The contribution of the article is to present the first vehicle mobility dataset in the Gulf region by analysing the GPS-based vehicle mobility data collected from eight participants using telematics devices for 15 months. Even though the number of participants is limited due to the conservativeness of the Gulf community, this is the first study in a carbon-rich developing country which provides insights into distinctive driving patterns in such countries. The gathered mobility data is processed to analyse their daily trip characteristics on weekdays and weekends, including the time they depart from or arrive at home, trip distances, etc., which are then generalised for the entire vehicles in a particular community in Qatar. The habitual departure time which has the circular nature is depicted by a mixture of von Mises (VM) models, while the distribution of non-negative time durations that vehicles spend away from (or park at home) conditioning on the hourly segmented departure (or arrival) time is simulated by combining truncated positive normal (TPN) models. Furthermore, given the same segmented departure time, the conditional distribution of daily trip distances is also fitted by mixed TPN models and then linked with the outdoor duration via the Clayton Copula. Then the MCMC method is applied to randomly generate vehicles' daily trip sequences which start from the VM-based departure time samples and move to subsequent arrival time and so on according to the associated TPN distributions of outdoor or home parking durations. The accompanying daily trip distances correlated with outdoor durations are also sampled to estimate the equivalent energy usages in hot weather conditions in Qatar. In this way, the proposed probabilistic method for vehicle data generalisation fully reflects the dependencies of daily trip attributes. Then the vehicles' daily trip sequences are translated into their domestic charging profiles, based on which the suitability of home charging for EV adopters and the predictability of community-scale EV charging demands are evaluated and compared between the uses of different charge rates. In addition, a probabilistic assessment method is developed in conjunction with power flow studies to statistically quantify the impacts of the community-scale EV integration on the local network voltage and thermal stability in numerous daily scenarios. A flow chart describing the processes of vehicle data generalisation and network stability assessment is shown in Fig. 1.

The article is structured as follows: Section II describes the collection and analysis of vehicle mobility data; Section III introduces the probabilistic methods for daily trip sampling and network integration assessment; Section IV validates the vehicle data generalisation and assesses the network stability with EV integration; and Section V presents conclusions and recommendations for further work.

II. GPS-BASED VEHICLE MOBILITY DATASET

A. VEHICLE MOBILITY DATA COLLECTION

High resolution vehicle mobility data is collected from 8 participants in Doha, Qatar form 10/05/2021 to 09/08/2022 using Teltonika Fm3001 on-board diagnostic (OBD) devices [14],

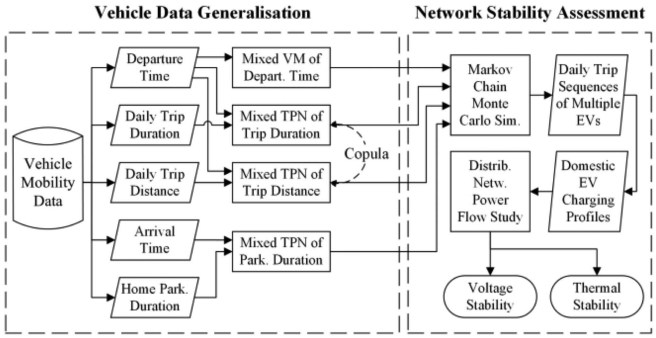

FIGURE 1. Processes of vehicle data generalisation and electric network stability assessment.

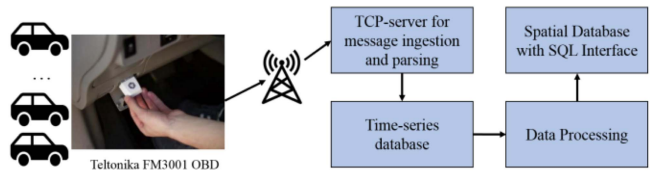

FIGURE 2. Schematic of vehicle mobility data acquisition system.

as shown in Fig. 2. The Teltonika OBD devices work on a specific Transmission Control Protocol (TCP) and deliver a variety of mobility data collection including vehicle speed, acceleration, GPS location, trip length, etc. to an on-premise server. Then the telematics data is ingested into a time-series database using InfluxDB [15] which can handle 100000 writes per second on a regular 2-core machine, permitting the data acquisition from all the Teltonika OBD devices. To alleviate the burden of data collection and ingestion, the data transfer is optimised by configuring a set of data processing rules within the Teltonika OBD devices: (i) if the duration between two consecutive timestamps is shorter than or exceeds 10 seconds, the vehicle is deduced to be moving or parking respectively; and (ii) a new trip is assumed to start only when the duration difference is greater than 10 seconds [12]. Furthermore, the spatial location data collected from the vehicles are clustered to analyse the location-based activities performed by the residents and detailed analysis is reported in our previous work [12].

B. VEHICLE MOBILITY DATA ANALYSIS

One of the primary focuses of this article is to examine whether home charging would be sufficient to charge EVs in Qatar. There are two key reasons to prioritise the assessment of home charging over public charging. First, the State of Qatar is located in a relative small region and almost all the residents are located in the capital city, Doha. Therefore, long-distance driving (e.g., interstate travel, etc.) is almost non-existing. Second, the car ownership level is very high as even multi-dwelling flats offer dedicated parking spaces for their residents. This is mainly because the country witnessed population growth over the last two decades and the building

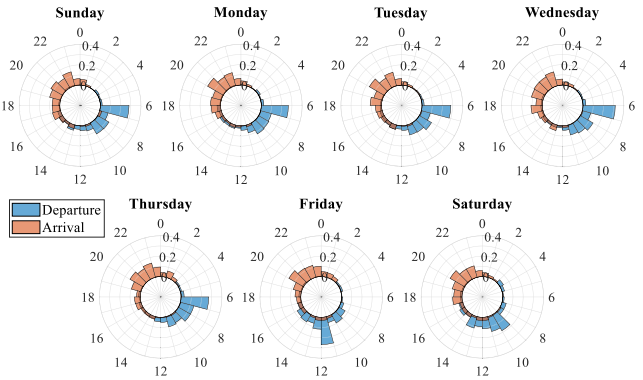

FIGURE 3. Relative frequencies of departure and arrival time observed on each day of a week.

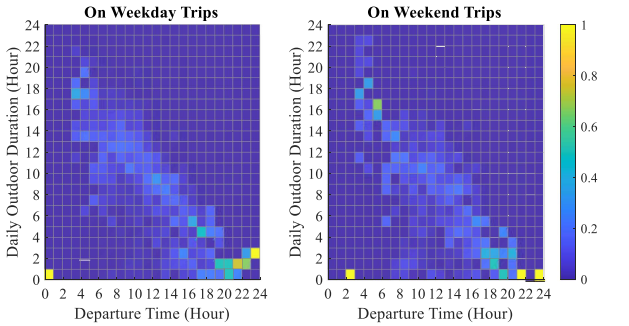

FIGURE 4. Relative frequencies of daily outdoor duration (hour) given different hourly segmented departure time on weekday and weekend trips.

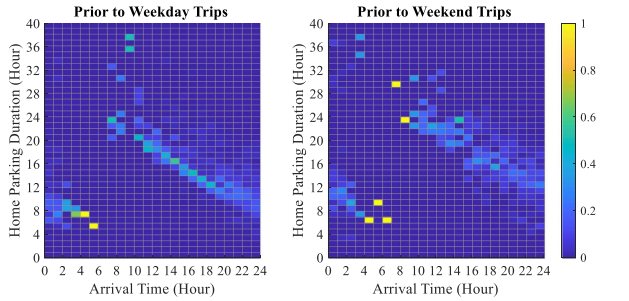

FIGURE 5. Relative frequencies of home parking duration (hour) given different hourly segmented arrival time before weekday and weekend trips.

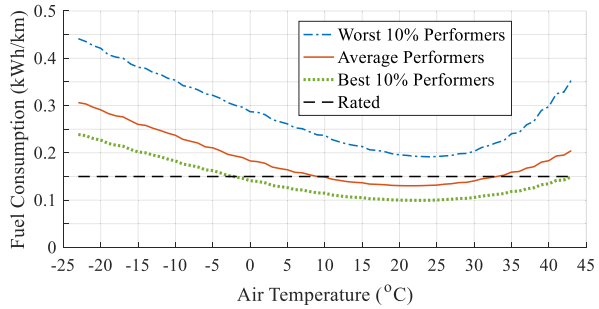

FIGURE 6. Temperature-dependent fuel consumptions (kWh/km) for 64 kWh Hyundai Kona under different driving performances.

stock is very young compared to other cities with high EV penetration [4]. To that end, our mobility analysis focuses on domestic charging and takes the Education City Community housing where university staffs are located [16].

The energy demand and load profiles of community-scale vehicle electrification is primarily characterised by their home parking durations and driving patterns. The former influencing factor can be estimated based on departure time from home and arrival time at home, which are, for brevity, referred to as departure time and arrival time, respectively. Fig. 3 shows the distributions of departure and arrival time of the daily trips recorded on each day of a week. The overall driving behaviour is similar between weekdays (i.e., Sunday to Thursday in Qatar), mostly departing from home around 6 am–11 am and arriving at home around 7 pm–11 pm, which reveals that the home parking duration generally lasts about 7 hrs–15 hrs. The main behavioural differences between weekdays and weekends are reflected in the departure time, which is mostly distributed over 9 am–2 pm on weekends and also slightly varies between Friday and Saturday. The significant shift in driving behaviour from weekdays to weekends implies the necessity of modelling behavioural characteristics for weekdays and weekends separately.

Since the data is collected from 8 vehicles, due to limited volunteer size, statistical models require to be developed on top of the collected dataset to simulate and sample the driving behaviour of a larger population size [6]. The mutual relationship between departure and arrival time must be considered in the driving behaviour sampling process to avoid the creation of unrealistic daily trips such as excessive daily outdoor duration or short home parking duration. The heat maps in Figs. 4 or 5 show relative frequencies of the daily outdoor or home parking duration that starts from each hour of a day on or prior to weekday and weekend trips, respectively. The daily outdoor duration or the home parking duration generally reduces with the departure time increasing clockwise from 3 am or with the arrival time increasing clockwise from 7 am, respectively, providing a basis for the sequential sampling of departure and arrival time. In addition, the distributions of daily outdoor durations on weekday trips and home parking durations prior to weekday trips are more concentrated than those recorded for weekend trips.

To evaluate the charging energy requirements after daily trips, the daily trip distance (in km) of the participants are translated into their equivalent energy usage (in kWh) using a set of temperature-dependent fuel consumption curves (see Fig. 6) that are formed for 64 kWh Hyundai Kona based on real-world EV data differentiated by driver performance [17]. The EVs with 64 kWh batteries are particularly chosen here since the hot and arid desert climate in Doha [18] induces an extensive need of indoor and outdoor air-conditioning, which makes most residents prefer to use vehicles with high engine volumes (e.g., SUVs with 3.0+ engines) and require higher battery capacities to provide the same level of comfort [19]. (High-end EV models such as Mercedes EQS or Audi e-tron

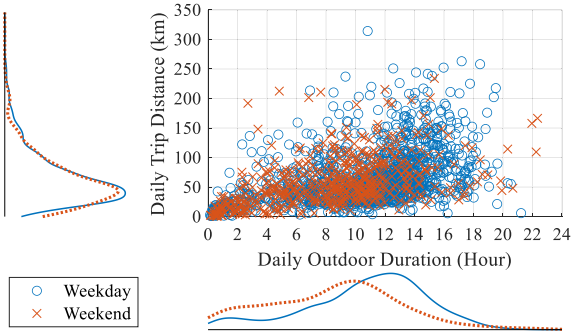

FIGURE 7. Data pairs of daily outdoor durations (hour) and trip distances (km) recorded on weekdays or weekends.

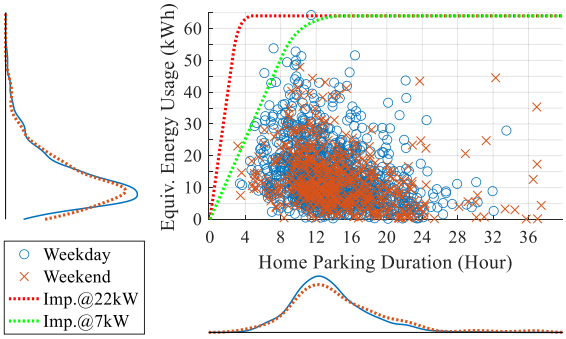

FIGURE 8. Data pairs of daily equivalent energy usages (kWh) and subsequent home parking durations (hour) prior to next weekday or weekend trips against the energy import (kWh) at a 22 kW or 7 kW nominal charge rate.

could also be possible alternatives to replace high-engine vehicles in the Gulf region, though the publication of their battery ranges under hot weather is required for related suitability studies). In addition to the driver performance and EV designs (e.g., weight, shape, etc.), ambient temperature can influence the fuel consumption (kWh/km) of an EV. As shown in Fig. 6, the average fuel consumption could be about 87% of the rated level only at an optimal temperature of 21 °C–22 °C and increase with the temperature approaching the extremely hot or cold conditions where the battery energy would be additionally consumed for auxiliary cooling or heating to keep the EV cabin and itself at a comfortable temperature [17]. Considering that the summer temperature can reach up to 50 °C in Doha, the average fuel consumption at 43 °C in Fig. 6 is adopted here to evaluate the equivalent energy usages of vehicles from daily trip distances. While this would provide an average estimate on fuel consumptions during hot seasons, future enhancement is required to reflect time-varying temperature conditions and diverse driving performances and simulate their effects on fuel usages (with the possible use of interpolation for the temperature outside the range of Fig. 6).

Although the daily outdoor duration comprising travel and activity time cannot directly reflect the accompanying daily trip distance, the scatter plot of their data pairs in Fig. 7 indicates a certain positive relationship for both weekday and weekend rips. Furthermore, daily trip distances are shown to mainly distribute around 50 km with most extreme values exceeding 250 km or even 300 km in this work, though all these trip distances would be met by a fully charged 64 kWh EV. In addition, their daily equivalent energy usages are plotted against the subsequent home parking durations in Fig. 8. In general, the home parking duration of 7 hrs –15 hrs would require replenishing up to 30 kWh of energy for daily trip distances up to 150 km. Given a 22 kW or 7 kW nominal charge rate combined with a 90% charging efficiency, Fig. 8 also shows the energy that could be imported by an empty EV battery over the home parking duration under a constant current (CC)-constant voltage (CV) regulation [20], which mostly exceeds the daily equivalent energy usage (i.e., actual import required), especially when the home parking duration goes further. This highlights the possibility of exploiting the role of EV batteries in demand side management.

III. PROBABILISTIC MODELLING OF EV TRIPS AND NETWORK INTEGRATION

This section develops a MCMC-based method to sample the sequence of daily trips for multiple residents based on the overall driving behaviour generalised from the mobility data. The MCMC inputs comprising the marginal distributions of initial departure time and home parking durations as well as the joint distributions of daily outdoor durations and trip distances are detailed first, followed by simulating the community-scale EV demands and their integration with a particular 11 kV distribution network in Doha, Qatar.

A. INDEPENDENT DISTRIBUTION OF INITIAL DEPARTURE TIME

To start the sampling process from the first daily trips $d = 1$ (i.e., Sunday in this case) with a reasonable set of departure time $t_{d=1}^{Dep}$, the independent probability density function (PDF) $f_{vm}(t_{d=1}^{Dep}|\cdot)$ of the departure time observed on weekdays is modelled by a mixture of von Mises (VM) distributions [21], [22] which are the circular analogue of normal distributions and thus capture the circular nature of departure time:

$$f_{vm}\left(t_{d=1}^{Dep}|p_i,\mu_i,k_i\right)=\sum_{i=1}^{N_{vm}}p_i \cdot \frac{\exp\left(k_i\cdot\cos\left(\tau\left(t_{d=1}^{Dep}\right)-\mu_i\right)\right)}{2\pi\cdot I_0\left(k_i\right)} \quad (1)$$

where the operator $\tau(\cdot)$ converts $t_{d=1}^{Dep}$ from [00:00, 24:00) to $[-\pi, \pi)$; the term p_i $(i = 1, .., N_{vm})$ denotes the proportion of the i^{th} VM component which has an angular centre μ_i in $[-\pi, \pi)$ and a non-negative concentration k_i; and $I_0(\cdot)$ is the modified Bessel function of the first kind of order zero. The parameters (p_i, μ_i, k_i) of the mixture of VM distributions are estimated by the maximum likelihood estimation (MLE)

[23] based on the weekday departure time observations. To avoid an over- or under-fitting problem, the optimal number of VM components is determined by examining the Bayesian inference criterion (BIC) which indicates a trade-off between the number of free model parameters and the maximised likelihood $\hat{L}_{vm}$ [24], as formulated by (2) where M_{wd} is the number of weekday trip observations. The VM model with the number of mixtures leading to the minimum BIC will be adopted to depict the independent distribution of $t_{d=1}^{Dep}$.

$$BIC_{vm} = (3 \cdot N_{vm} - 1) \cdot \ln(M_{wd}) - 2 \cdot \ln\left(\hat{L}_{vm}\right) \quad (2)$$

B. CONDITIONAL DISTRIB. OF TEMPORAL AND TRIP DISTANCES

The temporal dependencies of daily trips performed by a residence are described here based on the conditional distribution of the arrival time t_d^{Arr} of the d^{th} daily trip given the upstream departure time t_d^{Dep} and the conditional distribution of the departure time t_{d+1}^{Dep} of the $(d+1)^{th}$ daily trip given the upstream t_d^{Arr}. The historic departure time observed on weekdays (or weekends) is first divided into hourly segments across 24 hours of a day, with the accompanying temporal distance (i.e., outdoor duration) to its subsequent arrival time being calculated and modelled by a mixture of TPN distributions $f_{tpn}^{D2A}(\cdot)$ which truncate the normal distributions to the non-negative side [25]:

$$f_{tpn}^{D2A}\left(T_{d_h}^{D2A}|q_j,\lambda_j,\sigma_j\right) = \sum_{j=1}^{N_{tpn}} \frac{q_j}{\sigma_j \cdot \Phi(\lambda_j)} \cdot \phi\left(\frac{T_{d_h}^{D2A}}{\sigma_j} - \lambda_j\right) \quad (3)$$

where $T_{d_h}^{D2A}$ is the temporal distance from the departure time $t_{d_h}^{Dep}$ within the h^{th} ($h = 1, \ldots, 24$) hourly segment on weekdays (or weekends) to its subsequent arrival time; q_j is the proportion of the j^{th} ($j = 1, \ldots, N_{tpn}$) TPN component with a shape parameter λ_j and a scale parameter σ_j; and $\phi(\cdot)$ and $\Phi(\cdot)$ are the PDF and cumulative distribution function (CDF) of the standard normal distribution respectively. The parameters $(q_j, \lambda_j, \sigma_j)$ of the mixture of TPN distributions are estimated by the MLE based on the temporal distances that accompany the $t_{d_h}^{Dep}$ observations. Then the optimal number of mixed TPN components is determined by minimising the BIC as formulated by (4):

$$BIC_{tpn} = \left(3 \cdot N_{tpn} - 1\right) \cdot \ln\left(M_{d_h}\right) - 2 \cdot \ln\left(\hat{L}_{tpn}\right) \quad (4)$$

where M_{d_h} and $\hat{L}_{tpn}$ denote the number of $t_{d_h}^{Dep}$ observations and the maximised likelihood of their accompanying temporal distances, respectively. Similarly, (3) and (4) can be used to estimate the distribution $f_{tpn}^{A2D}(\cdot)$ of the temporal distance $T_{d_h}^{A2D}$ (i.e., home parking duration) from the arrival time $t_{d_h}^{Arr}$ within the h^{th} hourly segment to its subsequent weekday (or weekend) departure time. Then the temporal distance distribution conditioning on the hourly segmented departure (or arrival) time can be translated into the conditional distribution of the subsequent arrival (or departure) time by adding the temporal distance onto the known departure (or arrival) time. In addition, considering the non-negativity of daily trip distances $D_{d_h}^{Dis}$, their distributions $f_{tpn}^{Dis}(\cdot)$ conditioning on the accompanying $t_{d_h}^{Dep}$ are also differentiated between weekdays and weekends and fitted by the mixed TPN models separately, with the model parameters being estimated in a similar way to those formulated by (3) and (4).

C. JOINT DISTRIB. OF OUTDOOR DURATION AND TRIP DISTANCE

Even though the conditional distributions of daily outdoor durations $\hat{f}_{tpn}^{D2A}(T_{d_h}^{D2A}|\cdot)$ and trip distances $\hat{f}_{tpn}^{Dis}(D_{d_h}^{Dis}|\cdot)$ are produced for the same hourly segmented departure time $t_{d_h}^{Dep}$ in Section III-B, the random samples produced from their respective marginal distributions cannot reflect the relationship between their historic observations as given in Fig. 7. The Copula function provides a way to describe the dependence structure between multiple random variables by modelling a joint distribution from their respective marginal distributions [26]. In order to introduce correlations into the random samples of $T_{d_h}^{D2A}$ and $D_{d_h}^{Dis}$, the Clayton Copula $C(\cdot)$ is used here to form their joint CDF by linking their marginal CDFs $\hat{F}_{tpn}^{D2A}(T_{d_h}^{D2A}|\cdot)$ and $\hat{F}_{tpn}^{Dis}(D_{d_h}^{Dis}|\cdot)$, with a focus on the modelling of their tail dependencies [26]:

$$C\left(T_{d_h}^{D2A},\ D_{d_h}^{Dis}\right) = \max\left(\hat{F}_{tpn}^{D2A}\left(T_{d_h}^{D2A}|\cdot\right)^{-\alpha} + \hat{F}_{tpn}^{Dis}\left(D_{d_h}^{Dis}|\cdot\right)^{-\alpha} - 1; 0\right)^{-1/\alpha} \quad (5)$$

where the parameter α is estimated by fitting $C(\cdot)$ to the empirical joint CDF of $T_{d_h}^{D2A}$ and $D_{d_h}^{Dis}$. Then the fitted $\hat{C}(\cdot)$ can be translated into a joint PDF by using:

$$\hat{f}_C\left(T_{d_h}^{D2A}, D_{d_h}^{Dis}\right) = \frac{\partial^2 \hat{C}\left(T_{d_h}^{D2A}, D_{d_h}^{Dis}\right)}{\partial \hat{F}_{tpn}^{D2A}\left(T_{d_h}^{D2A}|\cdot\right) \cdot \partial \hat{F}_{tpn}^{Dis}\left(D_{d_h}^{Dis}|\cdot\right)} \cdot \hat{f}_{tpn}^{D2A}\left(T_{d_h}^{D2A}|\cdot\right) \cdot \hat{f}_{tpn}^{Dis}\left(D_{d_h}^{Dis}|\cdot\right) \quad (6)$$

from which the conditional PDF $\hat{f}_C^{Dis}(D_{d_h}^{Dis}|\hat{T}_{d_h}^{D2A})$ of $D_{d_h}^{Dis}$ given an already sampled $\hat{T}_{d_h}^{D2A}$ can be derived, as formulated by (7), and used to generate the $\hat{D}_{d_h}^{Dis}$ samples that will be correlated with $\hat{T}_{d_h}^{D2A}$.

$$\hat{f}_C^{Dis}\left(D_{d_h}^{Dis}|\hat{T}_{d_h}^{D2A}\right) = \frac{\partial^2 \hat{C}\left(\hat{T}_{d_h}^{D2A}, D_{d_h}^{Dis}\right)}{\partial \hat{F}_{tpn}^{D2A}\left(\hat{T}_{d_h}^{D2A}|\cdot\right) \cdot \partial \hat{F}_{tpn}^{Dis}\left(D_{d_h}^{Dis}|\cdot\right)} \cdot \hat{f}_{tpn}^{Dis}\left(D_{d_h}^{Dis}|\cdot\right) \quad (7)$$

D. MCMC FOR DRIVING BEHAVIOUR SAMPLING

In order to incorporate the temporal dependency of daily trips into the driving behaviour sampling, the MCMC simulation [27], [28] which can sample multiple sequences of random

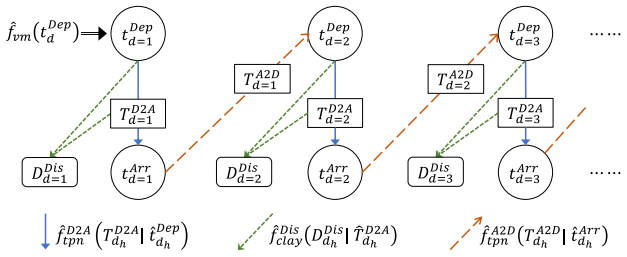

FIGURE 9. Process of MCMC simulation for daily trip sequence sampling.

TABLE 1. PV Capacities (MW), Peak Residential Demands (MW), and Numbers of EVs Connected at 11kV/0.415kV Substations

S/S Index	PV (MW)	Dem. (MW)	No. EVs	S/S Index	PV (MW)	Dem. (MW)	No. EVs
S1_1	0.04	1.397	24	S3a_2	0.04	1.187	9
S2_1	0.04	1.291	43	S3b_2	0.04	1.110	9
S3_1	0.04	1.097	9	S4_2	0.04	1.343	40
S4_1	0.04	1.353	23	S5_2	0.04	1.452	13
S5_1	0.04	1.155	41	S6_2	0.04	1.329	48
S6_1	0.04	1.479	24	S7_2	0.04	1.327	25
S1_2	0.04	1.495	25	S8_2	0.04	1.578	18
S2_2	0.04	1.183	5	S9_2	0.04	0.912	8

variables with the dependency of future states on current states is used here to randomly produce the arrival (or departure) time from its conditional distribution given the already sampled upstream departure (or arrival) time. Fig. 9 illustrates the process of the MCMC simulation for each driver which initiates with $t_{d=1}^{Dep}$ randomly sampled from $\hat{f}_{vm}(t_{d=1}^{Dep}|\cdot)$ and then moves to t_d^{Arr} and t_{d+1}^{Dep} progressively according to the associated temporal distance distributions $\hat{f}_{tpn}^{D2A}(T_{d_h}^{D2A}|\hat{t}_{d_h}^{Dep})$ and $\hat{f}_{tpn}^{A2D}(T_{d_h}^{A2D}|\hat{t}_{d_h}^{Arr})$ that are conditioning on the hourly segmented $\hat{t}_{d_h}^{Dep}$ and $\hat{t}_{d_h}^{Arr}$ respectively. Meanwhile, the travel distance D_d^{Dis} associated with a daily trip departing at $\hat{t}_{d_h}^{Dep}$ is randomly sampled from its Copula-based conditional distribution $\hat{f}_C^{Dis}(D_{d_h}^{Dis}|\hat{T}_{d_h}^{D2A})$ given the already sampled $\hat{T}_{d_h}^{D2A}$. In this way, the temporal relationship between departure and arrival time and the correlation between daily outdoor duration and trip distance are introduced into the driving behaviour samples.

E. DISTRIBUTION NETWORK WITH EV INTEGRATION

The community-scale vehicle electrification is simulated here in the context of the Education City Community, Doha, which is powered by the local 11 kV distribution network, as shown in Fig. 10. The network imports electricity from the upstream 66 kV grid and distributes across 11kV/0.415kV substations where 0.05 MW photovoltaic (PV) generators and residential housings are connected [29]. Table 1 tabulates PV generator capacities, peak residential demands and potential numbers of EVs that are integrated with different 11kV/0.415kV substations, totaling 0.64 MW, 20.686 MW

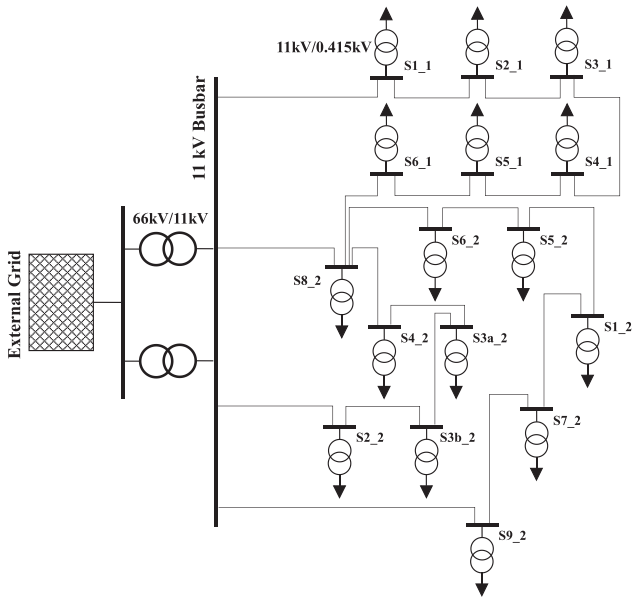

FIGURE 10. Local 11 kV distribution network supporting the education city community, Doha, Qatar.

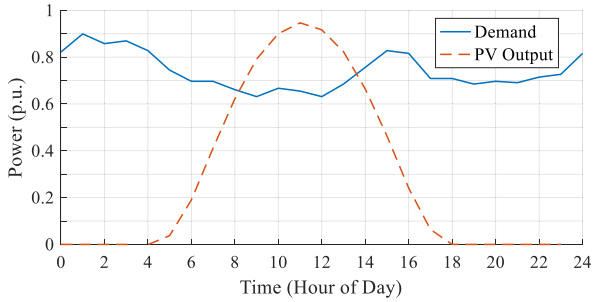

FIGURE 11. Typical daily profiles of normalised residential demands and PV power outputs in hot seasons.

and 364 EVs respectively. The time series of residential demands and available PV power outputs at each substation across 24 hours of a day are synthesised here based on their peaks and capacities in combination with their respective normalised typical daily profiles characterised for hot seasons, as shown in Fig. 11.

The driving behaviour of each EV is randomly produced by the MCMC simulation for 2×10^4 consecutive daily trips in order to ensure the convergence. The samples of daily trip distances are then translated into daily energy usages by the average fuel consumption at 43 °C in Fig. 6, based on which the energy left in EV batteries at the subsequent arrival time is updated. Then the charging profiles of EV batteries with a 90% charging efficiency are estimated to follow a 22 kW or 7 kW nominal rate under a particular CC-CV regulation [20] until it is fully charged or meets the subsequent departure time, depending on which comes first. Furthermore, it is assumed that the plugged EVs additionally consume 1.5 kW for continuous battery cooling (based on the heating demand study conducted in [30], which is assumed to be equivalent).

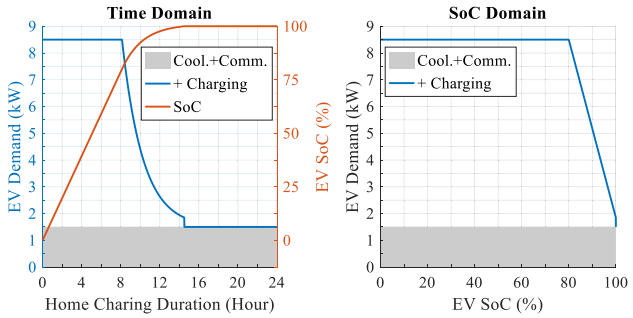

FIGURE 12. Demand curve (kW) of a drained EV under the 7 kW-based CC-CV regulation in time or SoC domain.

Fig. 12 shows a typical demand curve of a fully drained EV comprising the cooling and communication consumption and the 7 kW-based CC-CV charging profile in the time domain or the state of charge (SoC) domain respectively where the battery enters the CV stage when its SoC reaches 80% at around 8 hr. Finally, the power demands of EVs parking at home are added onto the net residential demands (i.e., the rises of existing residential demands above PV outputs), with their impacts on power flows and voltage profiles across the local network being quantified by solving the active and reactive power balance equations for all the network buses in each 15-minute period [31]:

$$P_b = \sum_{\beta=1}^{N_b} |V_b|\,|V_\beta|\left(G_{b\beta}\cdot\cos\Gamma_{b\beta} + B_{b\beta}\cdot\sin\Gamma_{b\beta}\right)\ \forall b \quad (8)$$

$$Q_b = \sum_{\beta=1}^{N_b} |V_b|\,|V_\beta|\left(G_{b\beta}\cdot\sin\Gamma_{b\beta} - B_{b\beta}\cdot\cos\Gamma_{b\beta}\right)\ \forall b \quad (9)$$

where V_b, P_b and Q_b are the voltage, net active and reactive power injected at the bus b ($b = 1, \ldots, N_b$), respectively; $G_{b\beta}$ and $B_{b\beta}$ are the real and imaginary parts of the element in the bus admittance matrix corresponding to the buses b and β; and $\Gamma_{b\beta}$ denotes the voltage angle difference between bus b and bus β. The power flows and voltage profiles across the network will be compared with the network capacities and voltage limits (i.e., 100%±5% of the nominal voltage levels) respectively to perform a steady-state evaluation on the feasibility of the community-scale vehicle electrification at the Education City Community.

IV. RESULTS AND MODEL VALIDATION

The driving behaviour modelling and the electric network simulation are carried out using MATLAB [32]. In addition, the electric network status with EV integration is estimated in conjunction with MATPOWER [33]. This section first validates the MCMC-based daily trip samples based on historic observations, and then evaluates the community-scale EV power demand profiles, followed by discussing their potential influences on the local network.

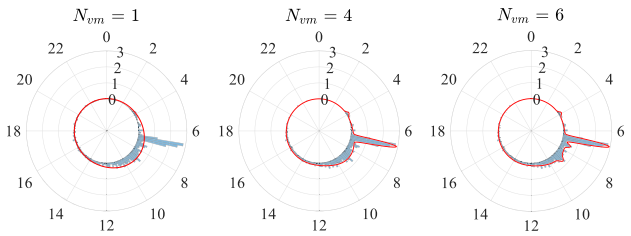

FIGURE 13. Independent PDFs of weekday departure time modelled by one, four and six VM components.

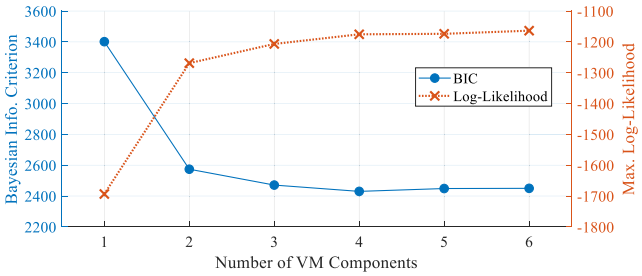

FIGURE 14. BIC and the maximised log-likelihood obtained by different numbers of VM components for the weekday departure time modelling.

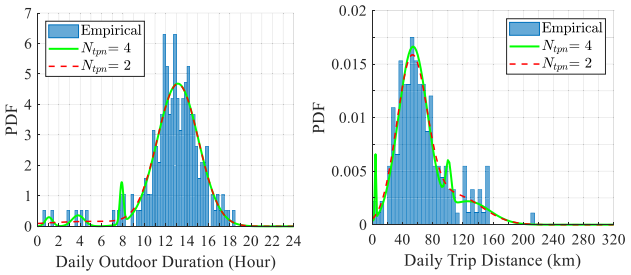

FIGURE 15. Empirical conditional distributions of daily outdoor durations (hour) and trip distances (km) of weekday trips departing over 8 am-9 am and their modelling by a mixture of two or four TPN components.

A. DETERMINATION OF MIXED VM AND TPN MODELS

Fig. 13 shows the independent distributions of weekday departure time fitted by one, four, and six VM components respectively. Although a higher number of VM components captures more departure time peaks and gives a better distribution fitting, the use of excessive VM components might cause an over-fitting problem and increase the BIC, as shown in Fig. 14. Therefore, a mixture of four VM components resulting in the smallest BIC with a reasonably high likelihood is adopted here to model the departure time distribution of the first daily trip.

The BIC level examination is also applied to different mixed TPN models which form the distributions of daily trip distance or temporal distance conditioning on each hourly segmented departure or arrival time. Although a mixture of three or four TPN components are required to provide a better fitting for some particular distributions, a single TPN or a combination of two TPN components is evaluated to achieve the lowest BIC for most distributions. For example, Fig. 15 shows the empirical and modelled conditional distributions of

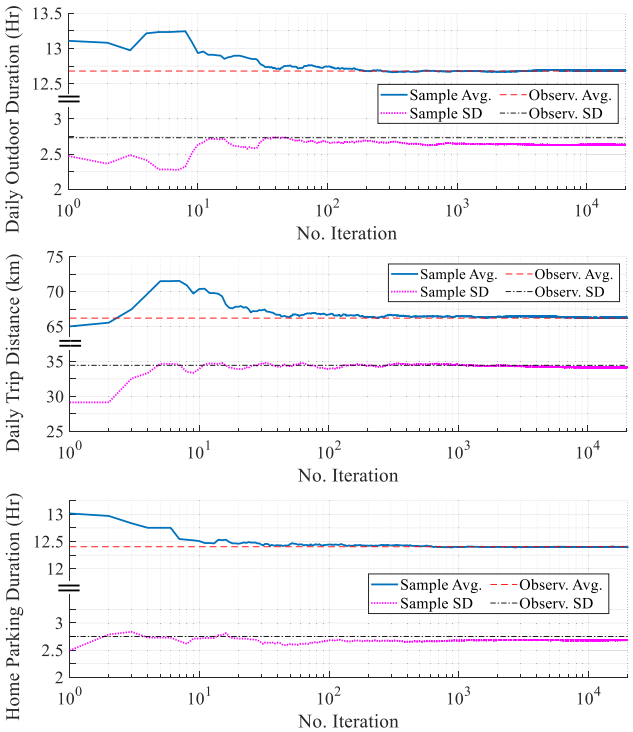

FIGURE 16. Convergence of averages and standard deviations of daily outdoor durations (hour) and trip distances (km) for weekday trips departing over 8 am–9 am and home parking durations (hour) starting over 8 pm–9 pm before weekday trips to their respective observation-based levels.

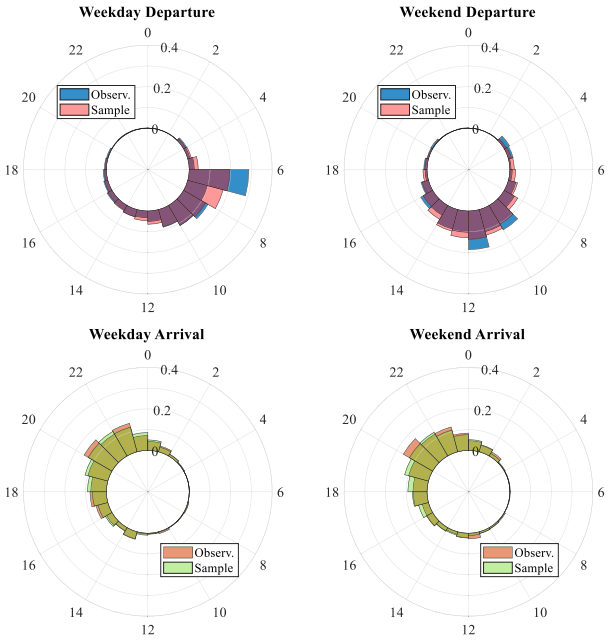

FIGURE 17. Distributions of MCMC samples or observations of departure and arrival time for weekday and weekend trips.

daily outdoor durations and trip distances respectively for the weekday trips that depart over 8 am–9 am. The use of four TPN components captures more data clusters and generates the log-likelihood values of about 171.8 for outdoor duration and −881 for trip distance, which are slightly greater than those that are achieved by mixing two TPN components, i.e., 165.6 and −884.8 respectively. However, the mixture of four TPN components using more parameters eventually leads to greater BIC levels (i.e., −286.3 for outdoor duration and 1819.3 for trip distance) than the use of two TPN components which has corresponding BIC levels of −305.1 and 1795.6. According to the indication of the BIC, the mixed TPN models having the best trade-off in the number of components are selected for the MCMC-based daily trip simulation.

B. VALIDATION OF DRIVING BEHAVIOUR SIMULATION

The driving behaviour sampled for the 364 vehicles over 2×10^4 daily trips (or iterations) are examined here to validate the effectiveness of the MCMC-based simulation. Fig. 16 show the variations of averages and standard deviations of outdoor durations and travel distances for weekday trip samples departing over 8 am–9 am and those of the home parking duration samples that start over 8 pm–9 pm prior to weekday trips respectively when the number of iterations increases towards 2×10^4. The averages and standard deviations gradually converge to their respective observation-based levels by up to 1 $\times$ 10^4 iterations and then stabilize till the end of 2×10^4 iterations. However, there still exists slight differences in standard deviations between samples and observations, mainly due to the fact that the associated conditional distributions are smoothed by the TPN models which aim to derive a general driving behaviour from the limited number of participants (see Fig. 15).

The smoothing effects of the mixed TPN models are also reflected in the distributions of departure and arrival time that are linked via temporal distance samples, as shown in Fig. 17 respectively. Although the MCMC samples reflect departure and arrival time distributions on average, especially the departure time shift between weekdays and weekends, they cannot fully depict some particular peak periods such as departure time clusters over 6 am–7 am on weekdays or 11 am–12 pm on weekends and arrival time clusters over 8 pm–9 pm. The issues associated with the smoothing effects can be addressed by generating MCMC samples from empirical distributions of temporal distances directly, though this would highlight the specific driving behaviour of the limited participants in the resulting MCMC samples. Provided with the collection of a sufficient number of daily trip data from diverse participants in further work, the mismatch between random samples and observations found here due to the smoothing effects could be mitigated.

In addition to linking departure time with arrival time, the daily outdoor duration sample itself must be correlated with the daily trip distance to reflect their relationship implied in observations. By employing the Copula to produce their joint distributions from observations, as shown in Fig. 18(a) for weekday trips departing over 8 am–9 am, the trip distance is

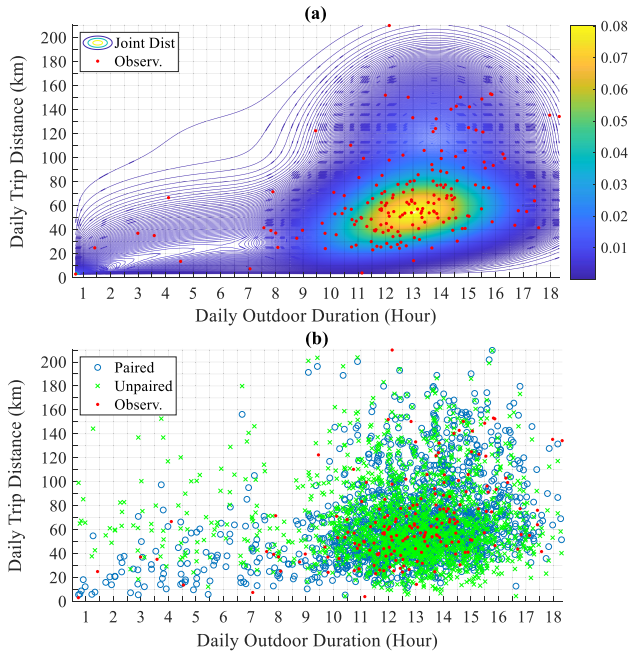

FIGURE 18. (a) Copula-based joint distribution of daily outdoor duration (hour) and trip distance (km) for weekday trips departing over 8 am–9 am and (b) the resulting sample pairs against the observations or unpaired samples.

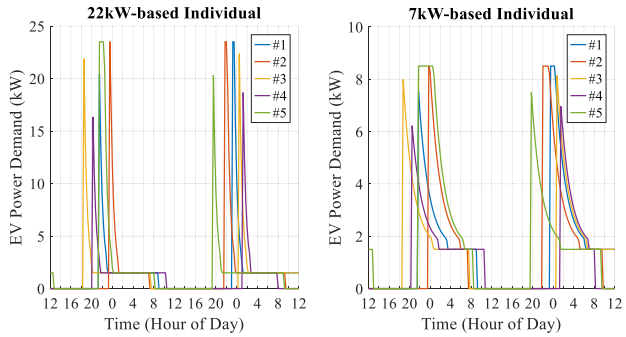

FIGURE 19. Individual demand profiles (kW) of five particular EVs over two consecutive simulation days based on 22 kW or 7 kW nominal charge rates.

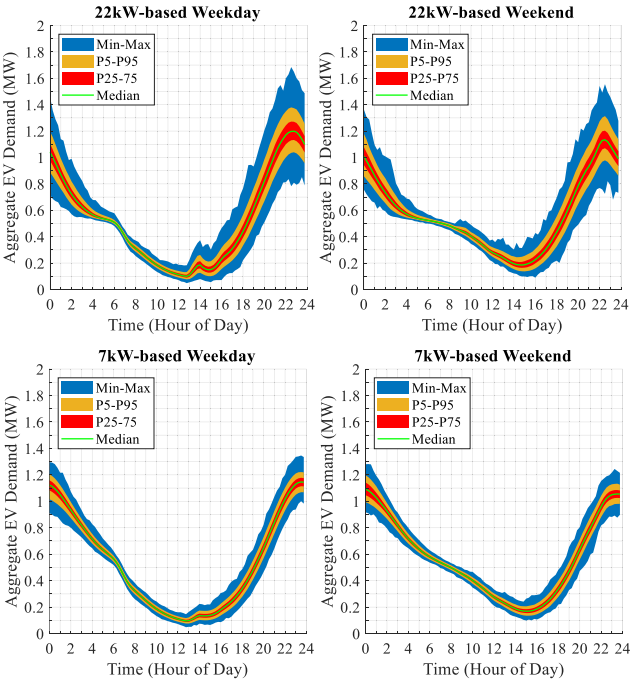

FIGURE 20. Distributions of EV demand profiles (MW) on weekdays and weekends under 22 kW or 7 kW nominal rates based on 30 simulation years.

randomly generated from its Copula-based conditional distribution given an already sampled outdoor duration. Fig. 18(b) shows that the Copula-based samples of outdoor duration and trip distance generally comply with the relationship of the observed data pairs. Compared with the unpaired samples of daily outdoor duration and trip distance which are independently produced from their respective marginal distributions and have a linear correlation coefficient of almost zero, the Copula-based sample pairs achieve a positive correlation coefficient of 0.32 which is close to the observed coefficient of 0.42. The slight difference in correlation coefficient is in part due to the smoothing effects of the Copula and the TPN models, as was noted above, and expected to be reduced with the number of daily trip records.

C. IMPACT OF EV INTEGRATION ON LOCAL NETWORK

Given that the MCMC process converges by up to 1×10^4 iterations (equivalent to about 30 simulation years) in this work, the daily trip sequences generated for the 364 EVs over 30 simulation years are translated into their respective demand profiles based on 22 kW or 7 kW nominal charge rates respectively, as shown in Fig. 19 for five particular EVs over two consecutive simulation days. The use of the 7 kW nominal rate is shown to cause a longer charging period, presenting a certain risk of not being fully charged before departure. It is evaluated that the EV batteries would reach at least 80% and 100% SoC before departure for 99.9% and 97.3% of daily trips respectively when the 7 kW nominal rate is adopted. For the use of the 22 kW nominal rate, the number of daily trips that the pre-departure SoC is lower than 80% or 100% is reduced to 0 or 3 out of about 4 million daily trips.

To understand the overall demand scale of the 364 EVs within the community, the distribution of their aggregate demands at each 15-minutes of a weekday or a weekend is estimated from the 30-year simulation, as shown in Fig. 20. The EV demand profiles generally increase with the EV arrival in the evening, and then decrease to around 0.55 MW which supplies the battery cooling for the 364 EVs before morning departure. When most of the EVs depart from home in the daytime, the aggregate EV demands continue dropping. Noticeable differences in EV demand profiles between weekdays and weekends are observed over 6 am–1 pm mainly due to the battery cooling and communication consumptions for the EVs that leave home later on weekends (see Fig. 17).

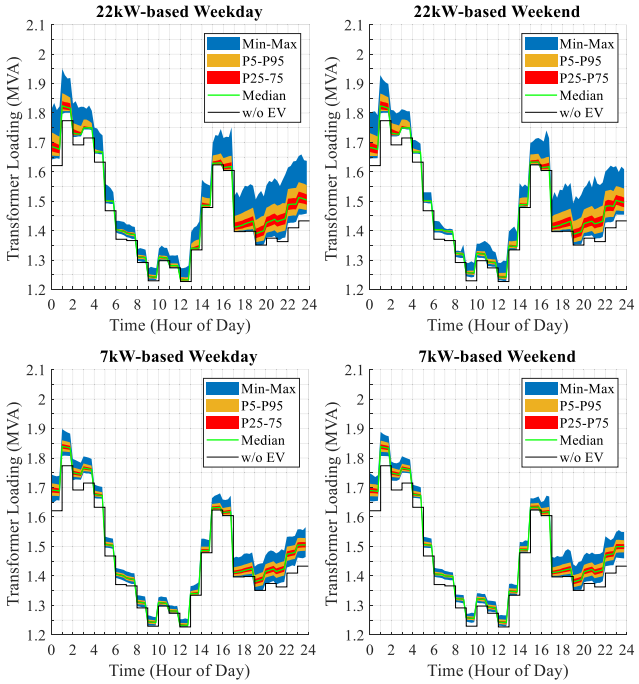

FIGURE 21. Distributions of the highest loads (MVA) on 11kV/0.415kV transformers at each 15-minutes of weekdays and weekends based on 22 or 7 kW nominal charge rates.

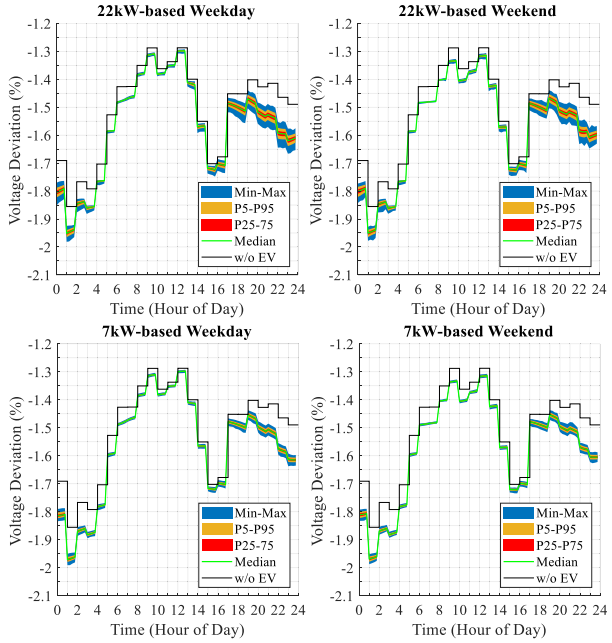

FIGURE 22. Distributions of the largest voltage deviations (%) on secondary sides of 11kV/0.415kV transformers at each 15-minutes of weekdays and weekends based on 22 or 7 kW nominal charge rates.

Furthermore, due to the non-concurrent charging phases of EVs, their aggregate demand profiles never exceed 1.7 MW (or 1.4 MW) which is equivalent to around 77 (or 200) EVs being simultaneously charged at 22 kW (or 7 KW) nominal rates. In addition, the aggregate EV demand distributions estimated based on the 7 kW nominal rates are more concentrated and thus more predictable than those for the 22 kW nominal rates, which will benefit the management of EV integration with local networks. Given the low probability of partial charge events in this work, the 7 kW nominal rates would be preferred for more predictable EV demands and reduced battery degradation [34].

In order to assess the potential impacts of EV integration on the local network, the individual demand profiles of the EVs connected to a common 11kV/0.415kV substation (see Table 1) are added onto the existing net demand profile of the substation to simulate steady-state power flows and voltage profiles across the network at each 15-minutes. Since the 11kV/0.415kV substations with 2.5 MVA transformers are the critical network branches that suffer from the severest voltage drops and the heaviest loads relative to branch capacities, the possible ranges of the highest loads and the greatest voltage deviations occurring at the 11kV/0.415kV transformers are estimated here for each 15-minutes of a weekday or a weekend based on the 30-year simulation, as shown in Figs. 21 and 22 respectively. Fig. 21 also shows the greatest transformer loading profile estimated without EV integration, compared with which the connection of EVs would increase the transformer loads by up to 0.2 MVA only. The relatively small load growths can not only be met by the capacity headroom of the transformers but will also lead to insignificant reductions in the secondary voltage levels of the transformers which are well kept within the 5% limits (see Fig. 22). Therefore, the community-scale vehicle electrification investigated here can be handled by the local network without reinforcements, especially when 7 kW nominal charge rates are selected.

V. CONCLUSION

The ability of electricity distribution networks to support local community-scale vehicle electrification must be assessed prior to deciding the network upgrades required to accommodate home charging electric vehicle demands. Accordingly, this article has developed a data-driven method to randomly sample daily trip sequences for the residential EVs based on the vehicle mobility data recorded by in-car diagnostic devices in Doha, Qatar. This particular case demonstrates learnings for regions where high per km energy consumptions of journeys may be common and will elongate peaks resulting from charging. The mixed von Mises models have been used to articulate the independent distribution of departure time from home due to its circular nature, whereas the distributions of daily trip distances and temporal distances between departure and arrival time conditioning on the hourly segmented departure or arrival time are fitted by the mixed truncated positive normal models due to their non-negativity. Furthermore, the correlations between daily trip distances and outdoor durations implied in historic records have been incorporated into their sample pairs via the Clayton Copula. In the main, the sequence of daily trip samples generated

through the Markov chain Monte Carlo process has reflected the average driving behaviour of the participants observed on weekdays and weekends. However, slight deviations still exist in the departure/arrival time distributions and the convergence of temporal/trip distances due to the smoothing effects of the mixture models which could be mitigated by fitting them to more vehicle mobility data measured from diverse drivers.

Based on 22 kW or 7 kW nominal charge rates combined with 1.5 kW additional consumptions for battery cooling and communication, the daily trip sequence samples comprising departure/arrival time and trip distance (or equivalent energy usage) over 30 simulation years have been converted into the power demand profiles for 364 EVs within a particular community. Compared with the 22 kW nominal rates which almost always allow EVs to be fully charged before departure, the 7 kW nominal rates would lead to a 100% pre-departure state of charge for around 97.3% of daily trips. However, the 7 kW nominal rates have reduced the demand magnitudes and increased the predictability of aggregate EV demand profiles, and would be preferable here from an EV battery health perspective. The reductions in EV demands have also alleviated the growths of power flows and voltage deviations at the critical branches within the local network which would accommodate the EV integration without reinforcements. This is mainly because the power networks in Qatar are recent installations which have enough spare capacity to host additional demands [35]. The power flow study was conducted here for the summer case to examine the worst-case scenarios. During mild winter months, the distribution network is not expected to be strained to the same extent as the load on the network is significantly lower than the summer season [35].

Provided with sufficient vehicle mobility data from diverse participants, the proposed data-driven methods for the driving behaviour modelling will be enhanced to distinguish the daily trip characteristics for each day of a week in future work. Furthermore, the mobility data for the vehicles within the community, together with the changes of EV fuel consumptions with time-varying air temperature and diverse driving performance of residents, will be considered to perform a more localised assessment on community-scale vehicle electrification. In addition, future work will exploit the role of EVs in demand side management by smoothing the power import from the upstream grid and/or reducing electricity costs for EV charging.

REFERENCES

[1] T. D. Güzel and K. Alp, "Modeling of greenhouse gas emissions from the transportation sector in Istanbul by 2050," *Atmospheric Pollut. Res.*, vol. 11, no. 12, pp. 2190–2201, Dec. 2020.

[2] G. Brückmann, F. Willibald, and V. Blanco, "Battery electric vehicle adoption in regions without strong policies," *Transp. Res. D: Transp. Environ.*, vol. 90, Jan. 2021, Art. no. 102615.

[3] H. F. Sindi, A. Ul-Haq, M. S. Hassan, A. Lqbal, and M. Jalal, "Penetration of electric vehicles in Gulf region and its influence on energy and economy," *IEEE Access*, vol. 9, pp. 89412–89431, 2021.

[4] E. S. Sahin, I. S. Bayram, and M. Koc, "Demand side management opportunities, framework, and implications for sustainable development in resource-rich countries: Case study Qatar," *J. Cleaner Prod.*, vol. 241, Dec. 2019, Art. no. 118332.

[5] G. Pareschi, L. Küng, G. Georges, and K. Boulouchos, "Are travel surveys a good basis for EV models? Validation of simulated charging profiles against empirical data," *Appl. Energy*, vol. 275, Oct. 2020, Art. no. 115318.

[6] Y. Wang and D. Infield, "Markov Chain Monte Carlo simulation of electric vehicle use for network integration studies," *Int. J. Elect. Power Energy Syst.*, vol. 99, pp. 85–94, Jul. 2018.

[7] Y. Xu, S. Çolak, E. C. Kara, S. J. Moura, and M. C. González, "Planning for electric vehicle needs by coupling charging profiles with urban mobility," *Nature Energy*, vol. 3, pp. 484–493, Apr. 2018.

[8] L. Kessler and K. Bogenberger, "Mobility patterns and charging behavior of BMW i3 customer," in *Proc. IEEE 19th Int. Conf. Intell. Transp. Syst.*, 2016, pp. 1994–1999.

[9] M. Wittmann et al., "A holistic framework for acquisition processing and evaluation of vehicle fleet test data," in *Proc. IEEE 20th Int. Conf. Intell. Transp. Syst.*, 2017, pp. 1–7.

[10] C. B. Harris and M. E. Webber, "An empirically-validated methodology to simulate electricity demand for electric vehicle charging," *Appl. Energy*, vol. 126, pp. 172–181, Aug. 2014.

[11] J. Fraile-Ardanuy, S. Castano-Solis, R. Álvaro-Hermana, J. Merino, and Á. Castillo, "Using mobility information to perform a feasibility study and the evaluation of spatio-temporal energy demanded by an electric taxi fleet," *Energy Convers. Manage.*, vol. 157, pp. 59–70, Feb. 2018.

[12] U. Zafar, I. S. Bayram, S. Bayhan, and R. Jovanovic, "Analysis of GPS-based high resolution vehicle mobility data towards the electrification of transportation in Qatar," in *Proc. IEEE 48th Annu. Conf. Ind. Electron. Soc.*, 2022, pp. 1–6.

[13] I. S. Bayram and S. Galloway, "Pricing-based distributed control of fast EV charging stations operating under cold weather," *IEEE Trans. Transp. Electrific.*, vol. 8, no. 2, pp. 2618–2628, Jun. 2022.

[14] Teltonika, *FM3001*. 2023. [Online]. Available: https://wiki.teltonika-gps.com/view/FM3001

[15] InfluxData, *InfluxDB Time Series Data Platform*. 2022. [Online]. Available: https://www.influxdata.com/

[16] O. Alrawi, I. S. Bayram, and M. Koc, "High-resolution electricity load profiles of selected houses in Qatar," in *Proc. IEEE 12th Int. Conf. Compat. Power Electron. Power Eng.*, 2018, pp. 1–6.

[17] Geotab, "To what degree does temperature impact EV range." 2023. [Online]. Available: https://www.geotab.com/uk/blog/ev-range/

[18] I. S. Bayram and M. Koc, "Demand side management for peak reduction and PV integration in Qatar," in *Proc. IEEE 14th Int. Conf. Netw. Sens. Control*, 2017, pp. 251–256.

[19] I. S. Bayram, "A stochastic simulation model to assess the impacts of electric vehicle charging on power generation: A case study for Qatar," in *Proc. IEEE Transp. Electrific. Conf. Expo.*, 2019, pp. 1–5.

[20] F. Fan, I. Kockar, H. Xu, and J. Li, "Scheduling framework using dynamic optimal power flow for battery energy storage systems," *Chin. Soc. Elect. Eng. J. Power Energy Syst.*, vol. 8, no. 1, pp. 271–280, Jan. 2022.

[21] J. Bentley, "Modelling circular data using a mixture of von Mises and uniform distributions," Ph.D. dissertation, Dept. Statist. Actuarial Sci., Simon Fraser Univ., Vancouver, BC, Canada, 2006.

[22] B. Stephen, S. Galloway, and G. Burt, "Self-learning load characteristic models for smart appliances," *IEEE Trans. Smart Grid*, vol. 5, no. 5, pp. 2432–2439, Sep. 2014.

[23] S. R. Eliason, *Maximum Likelihood Estimation: Logic and Practice*. Newbury Park, CA, USA: Sage, 1993.

[24] P. Stoica and Y. Selen, "Model-order selection: A review of information criterion rules," *IEEE Signal Process. Mag.*, vol. 21, no. 4, pp. 36–47, Jul. 2004.

[25] H. J. Gómez, N. M. Olmos, H. Varela, and H. Bolfarine, "Inference for a truncated positive normal distribution," *Appl. Math. J. Chin. Univ.*, vol. 33, pp. 163–176, Jun. 2018.

[26] F. Durante and C. Sempi, "Copula theory: An introduction," in *Copula Theory and its Applications. Lecture Notes in Statistics*, P. Jaworski, F. Durante, W. Härdle, and T. Rychlik, Eds. Berlin, Germany: Springer-Verlag, 2010, pp. 3–31.

[27] D. van Ravenzwaaij, P. Cassey, and S. D. Brown, "A simple introduction to Markov Chain Monte-Carlo sampling," *Psychon. Bull. Rev.*, vol. 25, pp. 143–154, 2018.

[28] P. Marjoram, J. Molitor, V. Plagnol, and S. Tavaré, "Markov chain Monte Carlo without likelihoods," *Proc. Nat. Acad. Sci.*, vol. 100, no. 26, pp. 15324–15328, Dec. 2003.
[29] M. Z. C. Wanik, A. A. Jabbar, N. K. Singh, and A. P. Sanfilippo, "Comparison on the impact of 0.4 MW PV with central inverter vs string inverter on distribution network operation," in *Proc. IEEE 7th Int. Conf. Power Energy*, 2018, pp. 162–167.
[30] D. Ramsey, A. Bouscayrol, and L. Boulon, "Energy consumption of a battery electric vehicle in winter considering preheating: Tradeoff between improved performance and total energy consumption," *IEEE Veh. Technol. Mag.*, vol. 17, no. 3, pp. 104–112, Sep. 2022.
[31] F. Milano, *Power System Modelling and Scripting*. Berlin, Germany: Springer-Verlag, 2010.
[32] *Matlab, MathWorks Introduces Release 2021a of MATLAB and Simulink*, 2021. [Online]. Available: https://www.mathworks.com/
[33] R. D. Zimmerman, C. E. Murillo-Sánchez, and R. J. Thomas, "MATPOWER: Steady-state operations, planning and analysis tools for power systems research and education," *IEEE Trans. Power Syst.*, vol. 26, no. 1, pp. 12–19, Feb. 2011.
[34] S. M. Bhagavathy, H. Budnitz, T. Schwanen, and M. McCulloch, "Impact of charging rates on electric vehicle battery life," *Findings*, vol. 2021, pp. 1–5, Mar. 2021.
[35] I. S. Bayram, F. Saffouri, and M. Koc, "Generation, analysis, and applications of high resolution electricity load profiles in Qatar," *J. Cleaner Prod.*, vol. 183, pp. 527–543, May 2018.